Supplementary Materials for

Emission of volatile organic compounds from petunia flowers is facilitated by an ABC transporter

Funmilayo Adebesin, Joshua R. Widhalm, Benoît Boachon, François Lefèvre, Baptiste Pierman, Joseph H. Lynch, Iftekhar Alam, Bruna Junqueira, Ryan Benke, Shaunak Ray, Justin A. Porter, Makoto Yanagisawa, Hazel Y. Wetzstein, John A. Morgan, Marc Boutry, Robert C. Schuurink, Natalia Dudareva*

*Corresponding author. Email: dudareva@purdue.edu

This PDF file includes:

Materials and Methods

Plant materials and growth conditions

Petunia hybrida cv. Mitchell diploid (W115; Ball Seed Co., West Chicago, IL) wild-type and transgenic plants were grown under standard greenhouse conditions with a light period from 6:00 h to 21:00 h. The *PhABCG1*-RNAi construct was generated as described previously (*21*) with some modifications. Briefly, to create a hairpin structure, DNA containing two spliced *PhABCG1* cDNA fragments corresponding to nucleotides 559-1071 and 559-871 (in antisense orientation) was synthesized (Genscript, Piscataway, NJ). Before synthesis, the Sol Genomics Network VIGS Tool (http://vigs.solgenomics.net/) (*30*) was used to verify that the designed *PhABCG1* dsRNA trigger would not result in off-target interference. The analysis was conducted by comparing the *PhABCG1* RNAi target sequence against the *Petunia axillaris* and *Petunia inflata* (parents of *Petunia hybrida*) (*31*) genomes using default parameters, except that the n-mer setting was adjusted to 24 nucleotides, which is generally considered to be below the threshold to efficiently trigger down regulation (*32, 33*). This analysis revealed that no other genes could be targeted by the *PhABCG1* dsRNA trigger. In addition, the maximum stretch of uninterrupted shared sequence with an off-target gene in our RNA-Seq dataset was found to be 16 nucleotides with *Ph19708* (fig. S15B). 5′-EcoRI and 3′-BamHI sites were introduced for directional cloning of the RNAi fragment into a pRNA69 vector containing the *Clarkia breweri linalool synthase* (*LIS*) petal-specific promoter (*25*) The resulting cassette containing the *LIS* promoter and the synthetic *PhABCG1* hairpin fragment was cut with NotI and SacI and subcloned into a pART27 simpler binary vector (*34*). *PhABCG1*-RNAi transgenic plants were generated via *Agrobacterium tumefaciens* (strain GV3101 carrying *PhABCG1*-RNAi) mediated transformation using the standard leaf disk transformation method (*35*) and 19 transgenic lines were screened for levels of *PhABCG1* mRNA and emitted VOCs.

RNA isolation and qRT-PCR analysis

Total RNA was isolated from wild-type and *PhABCG1*-RNAi petals (minimum of three flowers for each biological replicate) harvested at 15:00 h on day 2 post-anthesis using the Spectrum Plant Total RNA Kit (Sigma-Aldrich, St Louis, MO, USA). Total RNA samples were treated with DNaseI to eliminate genomic DNA using the RQ1 RNase-Free DNase kit (Promega, Madison, WI, USA) and were reverse transcribed to cDNA using the EasyScript cDNA synthesis kit (Applied Biological Materials Inc, Canada). *PhABCG1* mRNA expression was analyzed relative to the reference gene *UBQ10* (ubiquitin 10) by qRT-PCR as previously described (*36*). Gene specific primers for *PhABCG1* were 5′-TGGCGGATTTTTTCGATTAC-3′ and 5′-ACTCGTTCTTGAACATCCCTTCA-3′ and for *UBQ10* were 5′-GTTAGATTGTCTGCTGTCGATGGT-3′ and 5′-AGGAGCCAATTAAAGCACTTATCAA-3′. Final concentrations for all primers in each individual reaction were 300 nM. Each data point represents an average of three independent biological samples. To verify that expression of *Ph19708* was not affected by the *PhABCG1* RNAi construct, the following forward and reverse gene-specific primers were used to check *Ph19708* expression by qRT-PCR: 5-GCCAACTTCACAACGCAAAG-3' and 5-ATCCCAAATCGCGGAACAT-3'. Indeed, *Ph19708* expression was unchanged in *PhABCG1*-RNAi lines (fig. S15C).

Targeted metabolite profiling

Emitted volatiles were collected from detached flowers of wild-type and *PhABCG1*-RNAi transgenic lines (three flowers per biological replicate) from 18:00 h to 22:00 h on day 2 post-anthesis using a headspace method and analyzed by gas chromatography-mass spectrometry (GC-MS) as previously described (*37*). To determine internal pools of volatiles, 0.5 g of petal tissue was collected at 22:00 h, frozen in liquid nitrogen, ground to a fine powder and internal pools were extracted by dichloromethane for ~12 hs with shaking at 4°C. Samples were concentrated under a stream of nitrogen gas and analyzed by GC-MS as described previously (*38*). For alcohol glycosides, ~0.3 g of petal tissue collected at 22:00 h was ground to a fine powder in liquid nitrogen and extracted with 3 mL MeOH overnight at -20°C. Samples were centrifuged at 2500 x *g* for 5 min and supernatant was dried with a SpeedVac. Dry samples were resuspended in 1 mL phosphate-citrate buffer (100 mM, pH 5) and 200 µL Viscozyme® L (Sigma-Aldrich, St Louis, MO, USA) was added before covering with 500 µL of hexane. Samples were incubated at 37°C overnight with a gentle shaking (120 rpm). Samples were extracted with additional 500 µL hexane containing internal standard and analyzed by GC-MS.

Propidium iodide and fluorescein diacetate staining

Petals of wild-type and *PhABCG1*-RNAi flowers collected at 3 PM on day 2 post-anthesis were incubated in propidium iodide solution (10 µg/mL, Invitrogen, Carlsbad, CA) at room temperature for 1 h with shaking. Confocal fluorescence microscopy was carried out as described previously (*39*) with some modifications. Briefly, a Yokogawa spinning disk CSU-XI confocal head (Yokogawa Electric Corporation) mounted on a Zeiss Observer.Z1 inverted microscope was used to perform confocal fluorescence microscopy. A 20X PlanApo 0.8 NA dry-immersion objective was used. Propidium iodide was excited by a 561 laser and images acquired through a 617/73 emission filter. To mimic the toxicity of VOCs accumulated within the cell, wild-type petunia petals, collected at 9 AM on day 2 post-anthesis were fed with the range of concentrations (0, 3, 7.5, 15 and 30 mM) of benzaldehyde for 3 hours as described previously (*40*) with subsequent incubation with propidium iodide. After feeding the tissue was split in half and used for analysis of VOC internal pools and confocal microscopy. For fluorescein diacetate staining, petal tissues were incubated in fluorescein diacetate solution (50 µg/mL, Sigma-Aldrich, St Louis, MO, USA) at 4°C for 30 min with shaking, followed by gentle rinsing with water three times and confocal microscopy was performed as described above. A 60X C-Apo 1.2 NA dry-immersion objective was used. Fluorescein was excited by a 488 laser and images acquired through a 525/50 emission filter. All images were captured with 20% laser power and 50 ms exposure time. Signal intensity values were analyzed using ImageJ (https://imagej.nih.gov/ij/).

Heterologous expression of PhABCG1

The coding sequence of *P. hybrida* ABCG1 (JQ088099) was amplified by PCR from genomic DNA using the forward primer 5'-GCGCC**ATCGAT**ACAAACCAATTACCAAACAAAGTGG-3', which introduced a *Cla*I restriction site (shown in bold) and eliminated the initiating ATG codon for

translational fusion to an N-terminal 10His-StrepII tag, and the reverse primer 5'-CGCC**TTAATTAA**CTAGGAATCAAATACATCCAAAGG-3', containing a *Pac*I site (shown in bold). The amplified coding region was blunt-end cloned in pJET1.2/blunt vector (Thermo Fisher Scientific) and sequenced to verify that no error has been introduced during PCR amplification. The coding region was fused to an amino-terminal 10His-StrepII tag followed by a tobacco etch virus protease cleavage site (fig. S4) and transferred to a pAUX3131 vector (*41*) between the En_2PMA4 strong constitutive promoter and the tNOS terminator (*42*). The cassette was inserted in a pPZP-RCS2 vector (*41*) containing the kanamycin resistance gene *nptII*. The plasmid was linearized and used to transform *N. tabacum* cv. Bright Yellow 2 (BY-2) (*43*) suspension cells by biolistics. The BY-2 cell lines were cultivated as described by (*44*). Fifty kanamycin resistant clones were selected and screened for PhABCG1 expression by Western blotting of a microsomal fraction using the (Ni^{2+})-activated HisProbe-HRP (horseradish peroxidase) conjugate (Thermo Scientific).

Transport assays with BY-2 cells

Three days after dilution with a fresh MS medium, the BY-2 cell cultures were vacuum filtered on 3MM cellulose filters (Whatman^{TM}) using a 10-place filtration manifold (Hoefer, Inc.) and washed twice with 10 mL MS medium. The cells were subsequently resuspended at a density of 0.07 g cells/mL in the same medium and incubated for 150 min at 25°C. Four milliliters of the cultures were then transferred to 6-well plates (Greiner), placed under agitation (90 rpm) and 4 µL of radiolabeled substrates were added to the culture medium. The final concentrations of radiolabeled substrates were: 2 µM for [phenyl-^{14}C(U)]-methylbenzoate (39 mCi/mmol, Vitrax Co.), 1 µM for [phenyl-^{14}C(U)]-benzyl alcohol (55 mCi/mmol, Vitrax Co.), 50 nM for [1-^{3}H]-(±)-menthol (2 Ci/mmol, Vitrax Co.) and 5 µM for a sclareol analog [^{3}H]-decahydro-2-hydroxy-2,5,5,8a-tetramethyl-1-naphtalene ethanol (2 mCi/mmol - (*45*)). After incubation for the indicated periods of time, 1 mL of the cell culture was filtered on 3MM cellulose filters pre-wetted with 3 mL of ice-cold MS medium supplemented with 100 µM unlabeled substrate using a 10-place filtration manifold. Immediately after filtration, the cells were washed three times with the same medium, dried for 10 min at 37°C, and subsequently transferred to 3 mL of liquid scintillation fluid (Lumasafe, PerkinElmer) for radioactivity counting (Beckman LS 1701). The raw data, counts per minute (CPM), were converted to pmol.g^{-1}FW product based on specific activity of the substrate and efficiency of counting. For the inhibition studies, transport assays were performed as above with 2 µM [phenyl-^{14}C(U)]-methylbenzoate for 60 min in absence and presence of 500 µM vanadate, a phosphate analog that impairs ABC transport activity.

Preparation of microsomal and plasma membrane enriched fractions from BY-2 cells

Microsomal fractions from BY-2 suspension cells were prepared as described previously (*44*). The resulting microsomes were resuspended in suspension buffer (5 mM KH_2PO_4, 330 mM sucrose, 3 mM KCl, pH 7.8 (KOH), 1 mM phenylmethylsulfonylfluoride (PMSF), and protease inhibitor cocktail (leupeptin, aprotinin, antipain, pepstain and chymostain, each at 2 µg/mL) to a protein concentration of approximately 10 mg/mL. The samples were either frozen in liquid nitrogen and stored

4

at -80°C until further use or used directly for plasma membrane preparation. Plasma membranes were purified from 200 mg of a microsomal fraction by partitioning in an aqueous polymer two-phase system (*46*). The plasma membranes (approximately 1 mg of protein) were resuspended at 5 mg/mL in 10 mM Tris-HCl (pH 7.8), 330 mM sucrose and 0.1 mM Na$_2$EDTA, frozen in liquid nitrogen and stored at -80°C until further use.

Western blotting

Immunoblotting was performed as described previously (*20*). Briefly, after transfer of the proteins and blocking, the membranes were washed for 5 min and incubated either for 2 h with the (Ni^{2+})-activated HisProbe-HRP (horseradish peroxidase) conjugate (Thermo Scientific) or for 1 h with anti-H$^+$-ATPase primary antibodies followed by 1 h with HRP-conjugated anti-rabbit IgG antibodies. HisProbe-HRP was diluted at a ratio of 1:1,000, whereas anti-H$^+$-ATPase was diluted at 1:100,000 and anti-rabbit IgG at 1:10,000. After three 5 min washes, the antigen-antibody complexes were detected by the enhanced chemiluminescence method (Roche). The signals were recorded using a Kodak Image Station 4000R device.

Purification and gel filtration

The purification of PhABCG1 was adapted from (*47*). Microsomal proteins (400 mg) were solubilized with 0.5% dodecyl maltoside (DDM) at a detergent:protein ratio of 2:1 in solubilization buffer (20 mM Tris-HCl (pH 7.5), 50 mM NaCl, 20 mM imidazole, 10% (w/v) glycerol, protease inhibitors cocktail) for 30 min at 4°C under slow agitation. Non solubilized material was removed by centrifugation for 30 min at 100,000 *g*. One ml bed volume of Ni-NTA Agarose (Qiagen) previously equilibrated with the solubilization buffer supplemented with 0.03% maltose–neopentyl glycol (MNG) was added to the supernatant. After 2 h of incubation with slight agitation at 4°C (batch process), the resin was loaded in a chromatography column (Poly-Prep 20 mL, Bio-Rad), washed with 10 mL of washing buffer (20 mM Tris-HCl (pH 7.5), 50 mM NaCl, 20 mM imidazole, 10% (w/v) glycerol, 0.03% (w/v) MNG, protease inhibitors cocktail). Bound proteins were eluted with 3 mL of elution buffer (20 mM Tris-HCl (pH 7.5), 100 mM NaCl, 300 mM imidazole, 10% (w/v) glycerol, 0.03% (w/v) MNG, protease inhibitors cocktail) and desalted through a 5 mL Sephadex-G25 PD-10 column (GE Healthcare) equilibrated with 20 mM Tris-HCl (pH 7.5), 50 mM NaCl, 10% (w/v) glycerol, 0.03% (w/v) MNG). The resulting sample (4 mL) was concentrated by filtration through a Sartorius VivaSpin 2 filter (100 kDa cut off) to a final volume of 500 µL. The concentrate was loaded on a Superdex 200 Increase 10/300 GL (GE Healthcare) gel filtration column coupled to an ÄKTA Explorer (GE Healthcare) system. Proteins were eluted in 20 mM Tris-HCl (pH 7.5), 50 mM NaCl, 10% (w/v) glycerol, 0.03% (w/v) MNG at a rate of 0.4 mL/min. Protein absorbance was monitored at 280 nm and elution fractions of 1 mL were recovered and analyzed by immunoblotting.

Transient *PhABCG1* and *Ph5139* down-regulation

Transient down-regulation of *PhABCG1* and *Ph5139* was carried out as previously described (*48*). The *PhABCG*1-RNAi construct utilized for stable transformation (see above) was used for transient down-regulation. For the *Ph5139*-RNAi construct, a hairpin structure containing two spliced *Ph5139* cDNA fragments

corresponding to nucleotides 896-1400 and 896-1195 (in antisense orientation) were synthesized (Genscript, Piscataway, NJ) and inserted in the pENTR™/SD/D-TOPO® entry vector (Invitrogen, Carlsbad, CA). The resulting cassette was moved into the binary vector pB2WG7 with the Gateway™ LR Clonase™ II Enzyme Mix Kit (Invitrogen, Carlsbad, CA) and transformed into *Agrobacterium tumefaciens* strain GV3101. At least 20 one-day-old open wild-type petunia flowers were vacuum infiltrated with *Agrobacterium tumefaciens* strain GV3101 carrying either *PhABCG1*-RNAi, *Ph5139*-RNAi or the empty pB2WG7 vector (control). Volatiles were collected 2 days post-infiltration for 4 h from 18:00 h to 22:00 h and analyzed by GC-MS as described above. Internal pools of volatiles were extracted at 22:00 h and analyzed by GC-MS. *PhABCG1* and *Ph5139* expression was analyzed by qRT-PCR as described above. Samples for RNA extraction were harvested at 17:00 h 2 days post-infiltration. Specific primers for *Ph5139* were 5′- GTGACATTCTGGGCAGTTGG-3′ and 5′- TTCCCTGCCCAAAATGAAGC-3′.

Analysis of cuticle composition

For analysis of cuticular waxes, petals of wild-type and *PhABCG1*-RNAi day 2 post-anthesis flowers were dipped in 15 mL of GC-grade hexane for 30 s. Naphthalene was added as an internal standard, and the extracts were evaporated to dryness under a gentle stream of nitrogen gas. The dried residue was solubilized in equal amounts of BSTFA (*N*,*O*-bis(trimethylsilyl)trifluoroacetamide) and pyridine and heated at 100°C for 20 min. Excess BSTFA and pyridine was evaporated under N_2, then samples were solubilized in 200 µL of hexane and analyzed on a Agilent 7890A gas chromatograph equipped with a HP5-MS column (0.25 mm x 30m x 0.25µm, Agilent, Santa Clara, CA) and coupled to a 5975C inert MSD quadrupole mass spectrometer. The GC separation conditions were: an initial 2 min hold at 50°C, followed by a 40°C/min temperature ramp to 200°C and held for 10 min, then increased at 3°C/min to 280°C, and held at 280°C for 10 min. Compounds were identified based on retention times and fragmentation patterns and quantified by peak areas relative to the internal standard. Values are the average of three biological replicates each containing three flowers, and statistical comparison of identified peak amounts was determined by Student's *t*-test.

Transmission electron microscopy

Petals of wild-type and *PhABCG1*-RNAi day 2 post-anthesis flowers were immersed in fixative solution composed of 2.5% formaldehyde, 2.5% glutaraldehyde, 100 mM sodium cacodylate, pH 7.4 (Electron Microscopy Sciences, Hatfield, PA). After primary fixation, samples were washed with 0.1 M cacodylate buffer and post-fixed with 1% osmium tetroxide in 0.1 M cacodylate buffer, dehydrated in a gradient series of acetone, infiltrated and embedded in spurr resin. 70 nm thin sections were obtained with a Power Tome Ultramicrotome (RMC, Boeckeler Instruments. Tucson, AZ) and post-stained with uranyl acetate and lead citrate. Images were taken with JEOL 100CX Transmission Electron Microscope (Japan Electron Optics Laboratory, Japan) at an accelerating voltage of 100 kV.

Scanning electron microscopy

Petals of wild type and *PhABCG1-RNAi* day 2 post-anthesis flowers were sampled and prepared using methods described previously (*49*). Briefly, petals were fixed in 2% (v/v) glutaraldehyde in 100 mM cacodylate buffer pH 7.2, dehydrated in an ethanol series, and critical-point dried through carbon dioxide using a critical point drier (Autosamdri-931; Tousimis Research, Rockville, Maryland). Dried samples were mounted on aluminum stubs using carbon conductive tabs and sputter (208HR; Cressington, Watford, England) coated with gold. Samples were examined using a scanning electron microscope (Nova NanoSEM; FEI, Hillsboro, OR) at 5 kV.

Phylogenetic analysis

The complete amino acid sequences of 17 predicted PhABCGs and 21 functionally characterized plant ABCG transporters were aligned by Muscle using the MEGA6 software (*50*). The evolutionary history was inferred using the Neighbor-Joining method. The evolutionary distances were computed using the Poisson correction method and are in the units of the number of amino acid substitutions per site. Numbers at the nodes correspond to the percentage of 500 replicate bootstrap trees, which resolve the clade at the endpoints of that branch. The analysis involved 38 amino acid sequences. All ambiguous positions were removed for each sequence pair. There were a total of 1966 positions in the final dataset. Evolutionary analyses were conducted in MEGA6.

| A Contig_ID	Average FPKM in bud ± SD (Average CPM ± SD)	Average FPKM in day 2 flowers ± SD (Average CPM ± SD)	Fold change (edgeR FC)	FDR
PhABCG1	**1181 ± 452** **(10.7 ± 2.9)**	**121525 ± 14898** **(1345.5 ± 71.2)**	**102.9** **(124.1)**	**1.8E-158**
Ph5139	**5348 ± 1461** **(48.7 ± 8.5)**	**20192 ± 3056** **(224.5 ± 34.5)**	**3.8** **(4.6)**	**4.6E-25**
Ph15238a	15830 ± 4378 (144.0 ± 23.9)	17424 ± 1274 (193.4 ± 4.4)	1.1 (1.3)	7.4E-02
Ph9795	8814 ± 1018 (82.3 ± 17.1)	10003 ± 3224 (109.9 ± 30.1)	1.1 (1.4)	8.0E-02
Ph13519	9675 ± 1361 (88.9 ± 5.2)	6062 ± 2459 (66.2 ± 21.9)	0.6 (0.8)	7.4E-02
Ph20124	2114 ± 143 (19.5 ± 0.9)	1034 ± 188 (11.5 ± 1.8)	0.5 (0.6)	5.6E-04
Ph19962	1905 ± 258 (17.6 ± 2.6)	746 ± 114 (8.3 ± 1.7)	0.4 (0.5)	7.3E-07
Ph12412	1493 ± 307 (13.6 ± 1.3)	678 ± 38 (7.5 ± 0.2)	0.5 (0.5)	1.1E-04
Ph4681	**23 ± 3** **(0.2 ± 0.0)**	**623 ± 83** **(7.0 ± 1.3)**	**27.1** **(32.5)**	**1.1E-76**
Ph6796	1029 ± 158 (9.4 ± 0.5)	574 ± 86 (6.4 ± 1.1)	0.6 (0.7)	1.6E-02
Ph18683b	1182 ± 103 (11.0 ± 1.6)	511 ± 140 (5.6 ± 1.1)	0.4 (0.5)	1.2E-05
Ph15238b	8526 ± 845 (79.5 ± 15.4)	300 ± 58 (3.3 ± 0.5)	0.0 (0.1)	3.2E-85
Ph19708	2071 ± 182 (19.1 ± 0.4)	233 ± 35 (2.6 ± 0.4)	0.1 (0.1)	5.0E-38
Ph12172	504 ± 71 (4.6 ± 0.3)	139 ± 87 (1.6 ± 1.1)	0.3 (0.3)	9.7E-12
Ph18683a	265 ± 31 (2.5 ± 0.5)	131 ± 14 (1.5 ± 0.2)	0.5 (0.6)	1.2E-05
Ph3610	592 ± 252 (5.3 ± 1.7)	24 ± 6 (0.3 ± 0.1)	(0.1) (0.1)	3.3E-60
Ph21057	801 ± 87 (7.4 ± 0.1)	2 ± 3 (0.0 ± 0.0)	(0.1) (0.1)	2.1E-111
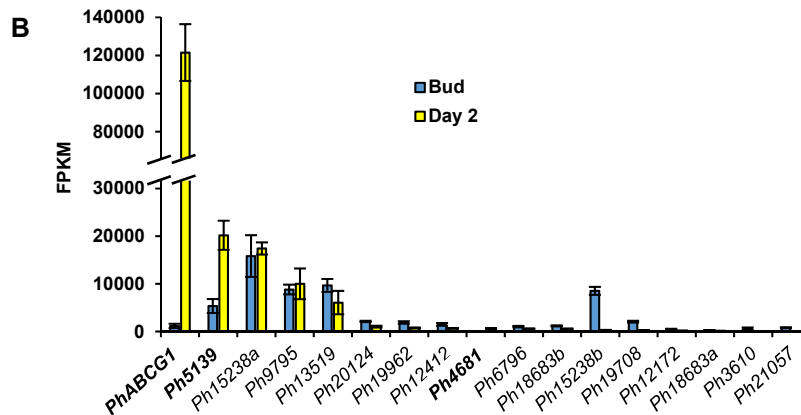
Fig. S1. ABCG transporter candidates identified in petunia RNAseq datasets. (**A**) Table and (**B**) graphical overview of expression of 17 *ABCG* transporter candidates at the bud stage and on day 2 post-anthesis. Gene expression was measured based on Cufflinks and edgeR analysis of RNAseq data (*21*). Data represent average of FPKM (fragments per kilobase per million mapped fragments) and CPM (counts per million reads) from three biological replicates ± SD. Table additionally contains average fold changes and FDR (false discovery rate) values from edgeR analysis (*21*). ABCG transporters significantly upregulated on day 2 versus bud stage are shown in bold.
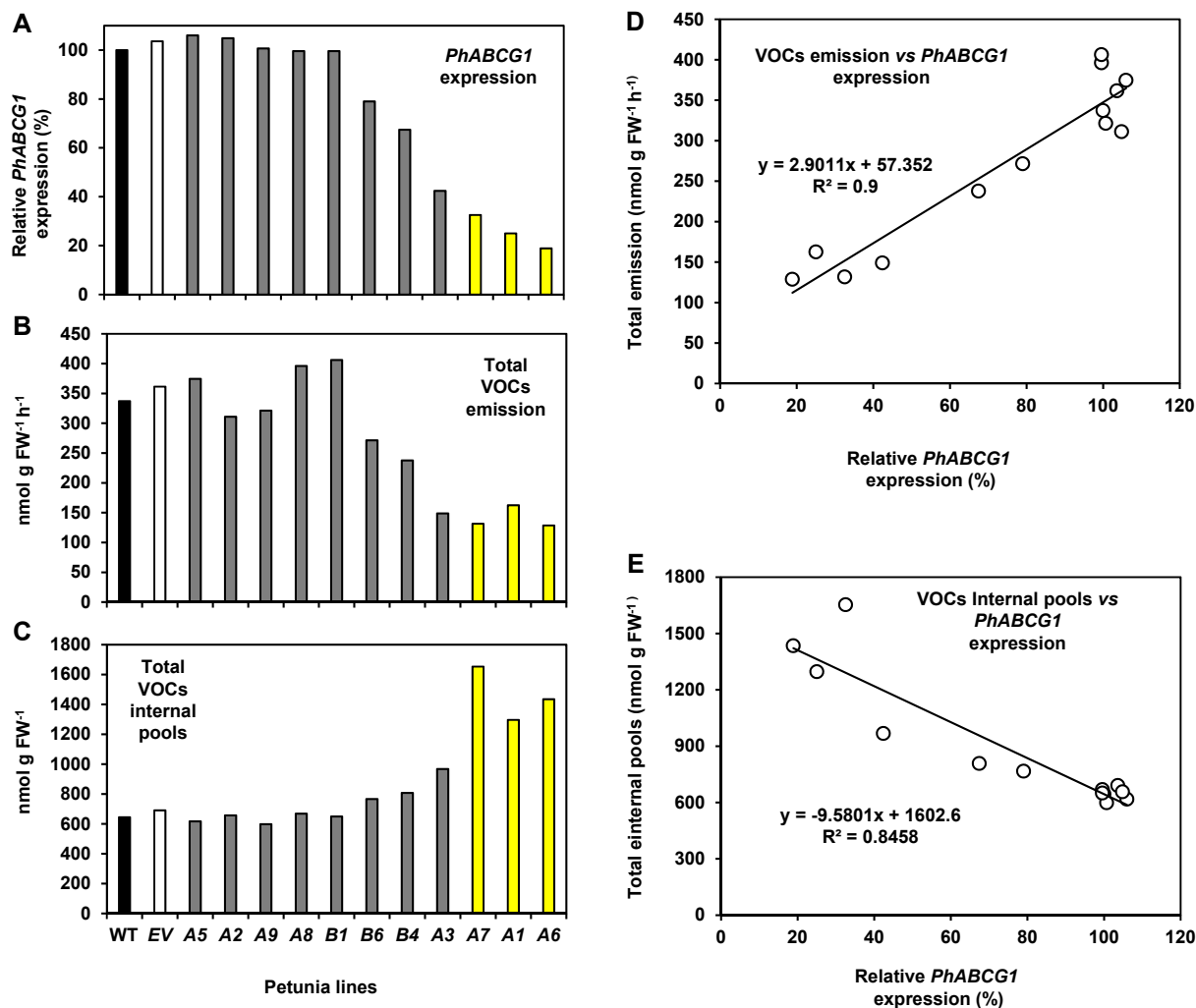
Fig. S2. Initial screening of PhABCG1-RNAi lines showing the correlation between *PhABCG1* expression and both emission and internal pools of volatiles. (A) *PhABCG1* mRNA levels determined by qRT-PCR on day 2 post-anthesis in wild type (WT), an empty vector (EV) transformed line and 11 independent *PhABCG1*-RNAi. (B) Total emission rate and (C) internal pools of volatiles from WT, empty vector transformed flowers and *PhABCG1*-RNAi flowers on day 2 post-anthesis. Volatile emission was measured from 18:00 h to 22:00 h. Internal pools were collected at 22:00 h. Correlation between the degree of *PhABCG1* down regulation and its effect on (D) VOC emission and (E) internal pools. RNAi lines used for detailed analysis are shown in yellow.
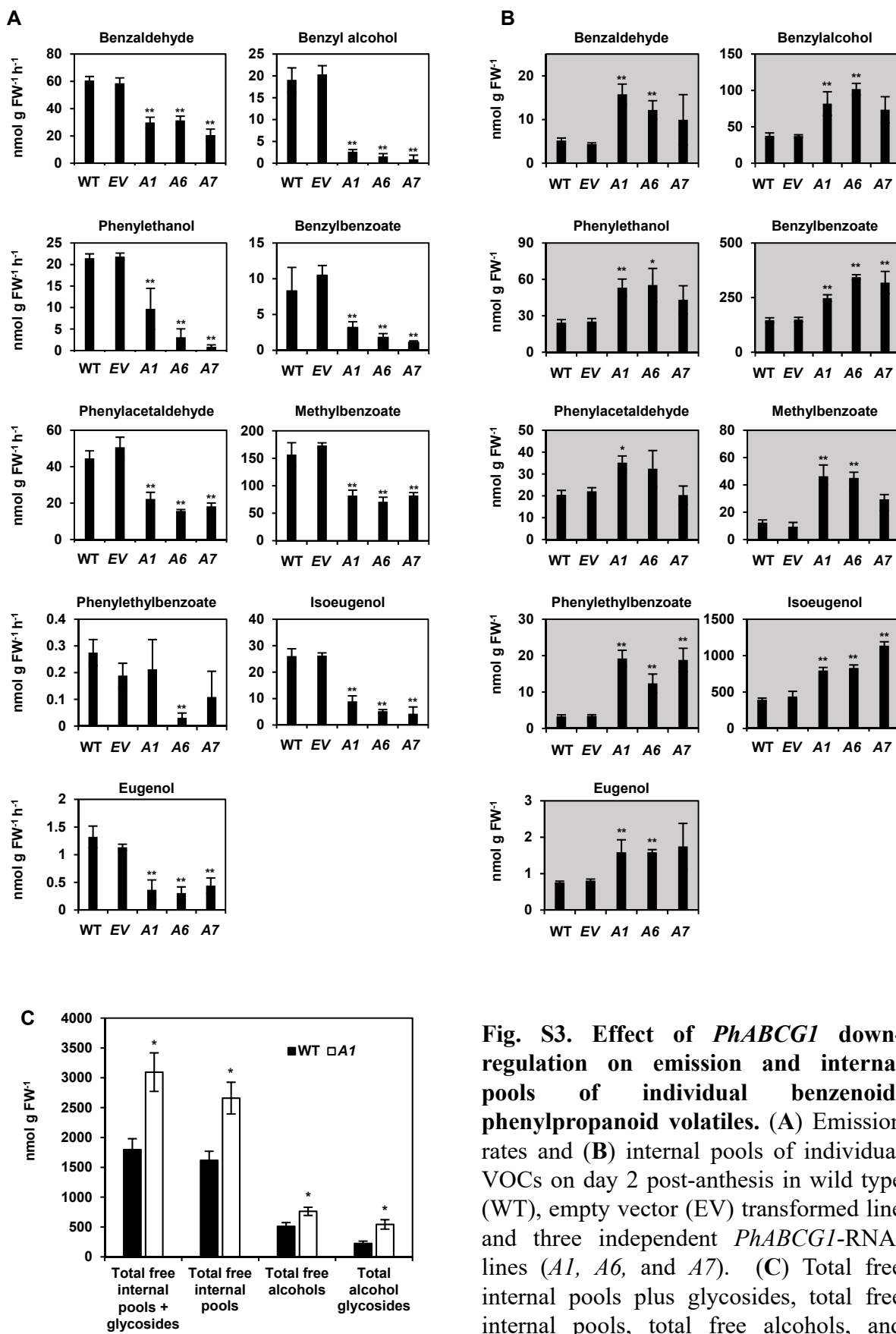
Fig. S3. Effect of *PhABCG1* down-regulation on emission and internal pools of individual benzenoid/phenylpropanoid volatiles. (**A**) Emission rates and (**B**) internal pools of individual VOCs on day 2 post-anthesis in wild type (WT), empty vector (EV) transformed line and three independent *PhABCG1*-RNAi lines (*A1, A6,* and *A7*). (**C**) Total free internal pools plus glycosides, total free internal pools, total free alcohols, and alcohol glycosides of petunia volatiles from WT and *PhABCG1*-RNAi flowers on day 2 post-anthesis. All data are means ± SEM (n=3 biological replicates). *P<0.05 and **P<0.01 by Student's *t*-test.

A

B

MSLGT<u>HHHHHHHHHH</u>GAG<u>WSHPQFEK</u>GAGTT<u>ENLYFQSG</u>TGAGAGARSID<u>TNQL</u>…

　　　　　　10 His　　　　　　　　StrepII　　　　　　　TEV　　　　　　　　ABCG1

C

5'-ATGTCACTGGGTACCCATCATCACCACCACCATCACCATCATCACGGTGCTGGATG
GTCACATCCACAATTTGAAAAGGGCGCTGGCACTACTGAGAACCTCTACTTCCAATC
TGGAACTGGTGCTGGCGCTGGTGCTAGATCT**ATCGAT**-3'

Fig. S4. Schematic representation of the construct used for *PhABCG1* overexpression in *Nicotiana tabacum* BY-2 cells. (**A**) The cassette contains the kanamycin resistance gene *nptII* (<u>Kana</u>[R]) between the constitutive promoter pNOS and the tOCS terminator (*39*), the fluorescence marker gene *mCherry* between the constitutive CaMV 35S promoter and the tNOS terminator and the *PhABCG1* coding sequence with a fused N-terminal His/StrepII tag under the control of the strong constitutive promoter En_2PMA4, 5' and 3' UTR from CPMV and the tNOS terminator (*42*). The entire 11,738 bp linear dsDNA fragment was used for transformation of *N. tabacum* BY-2 suspension cells by biolistics. (**B**) Amino acid sequence of the tag fused to the amino terminal end of PhABCG1. Underlined are the 10 Histidine tag, the StrepII tag, the sequence recognized by the tobacco etch virus protease (TEV) and the beginning of the PhABCG1 sequence. (**C**) Nucleotide sequence of the tag fused to the amino terminal end of PhABCG1. The *ClaI* restriction site is shown in bold,
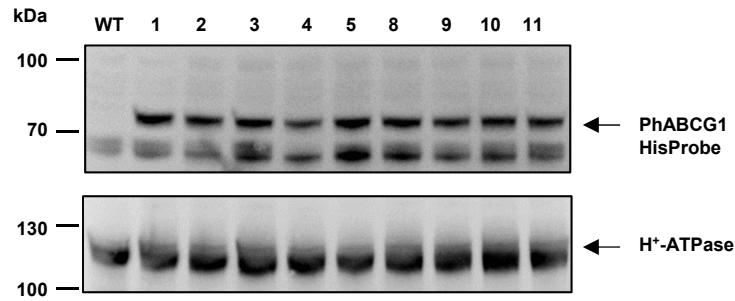
Fig. S5. Western blotting analysis of *Nicotiana tabacum* BY-2 cell lines expressing *PhABCG1*. Western blots were performed using 20 μg of protein from microsomal fractions prepared from wild type *N. tabacum* BY-2 (WT) and nine BY-2 lines expressing *His/StepII-PhABCG1*. Blots were probed with either HisProbe (upper panel) or anti-H$^+$-ATPase (lower panel) antibodies.
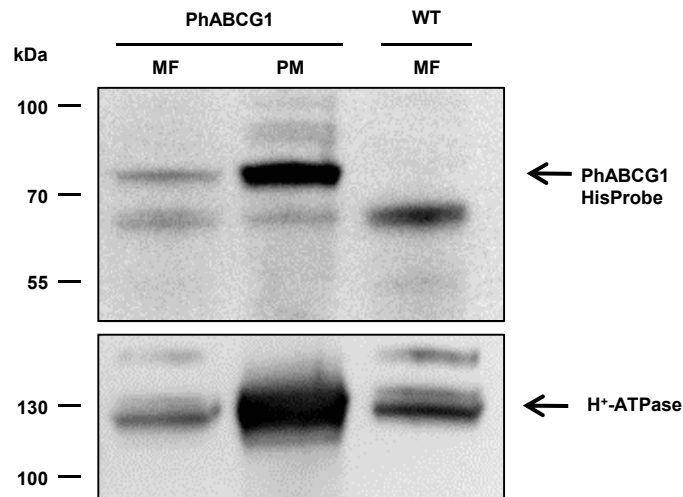

Fig. S6. Western blotting analysis of PhABCG1 enrichment in plasma membranes. Twenty μg of protein from microsomal (MF) and plasma membrane-enriched (PM) fractions prepared from the *PhABCG1*-expressing line 9 were analyzed by Western blotting using either HisProbe (upper panel) or an anti-H$^+$-ATPase antibody (lower panel). A wild type (WT) microsomal fraction was included as a negative control.
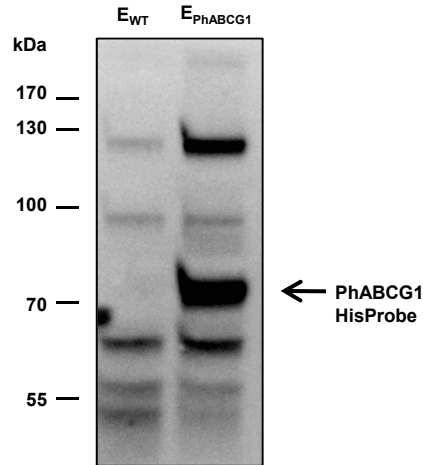
Fig. S7. Western blotting of partially purified PhABCG1 expressed in BY-2 cells. Microsomal fractions from a wild type BY-2 line (WT) and the *PhABCG1*-expressing line (*PhABCG1-9*) were solubilized with dodecyl maltoside and purified on an Ni-NTA column as indicated in Materials and Methods. The eluates of wild type (E_{WT}) and PhABCG1 ($E_{PhABCG1}$) were analyzed by Western blotting using HisProbe. The additional band corresponding to PhABCG1 is indicated with an arrow.
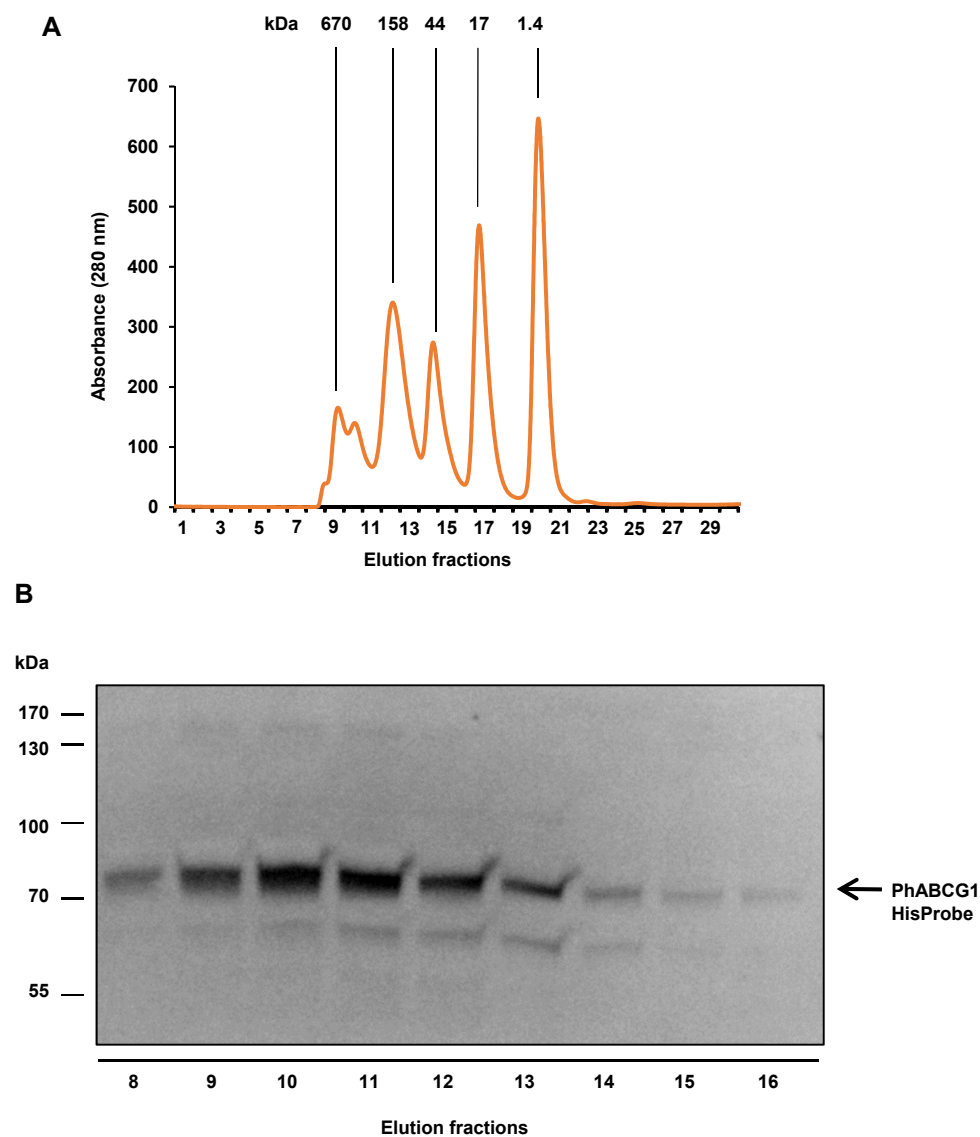
Fig. S8. Size exclusion chromatography analysis of PhABCG1. Partially purified PhABCG1 shown on fig. S7 was loaded on a Superdex 200 Increase 10/300 GL (GE Healthcare) column. (**A**) Elution of size markers with the indicated molecular mass. (**B**) The indicated fractions were analyzed by Western blotting using HisProbe.
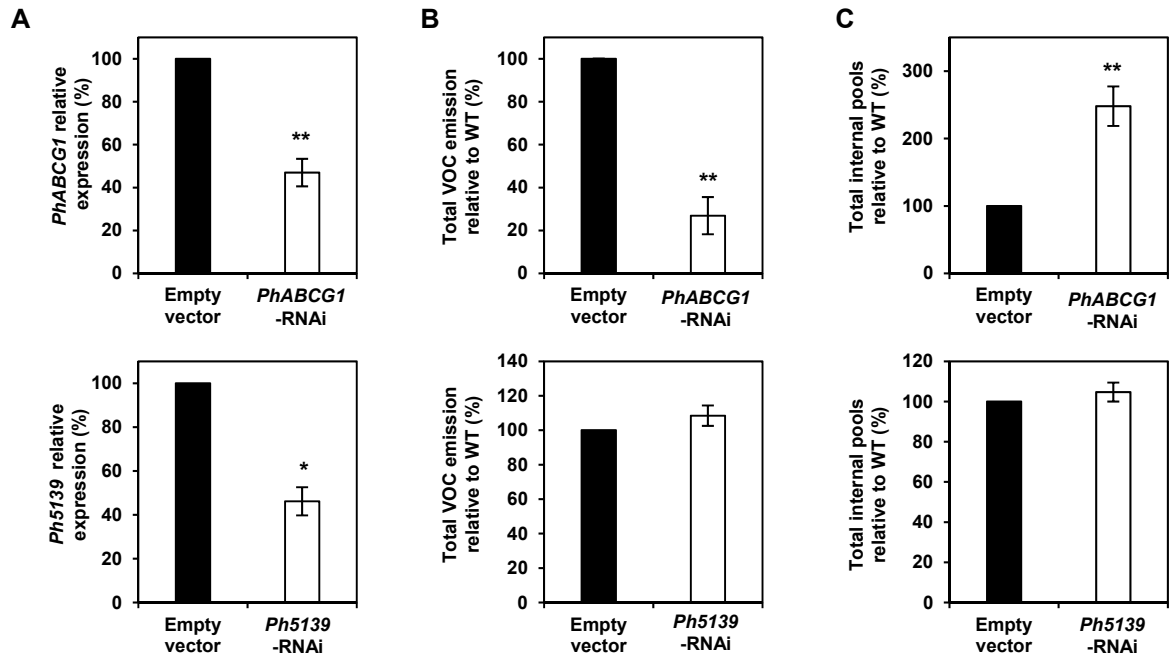
Fig. S9 Effect of transient _PhABCG1_ and _Ph5139_ down-regulation on VOC emission and internal pools in petunia flowers. Black and white columns represent flowers infiltrated with empty vector control or RNAi constructs, respectively. Upper panels, _PhABCG1_-RNAi used as a positive control; lower panels, _Ph5139-RNAi_. Transcripts levels (**A**), total VOC emission (**B**) and total VOC internal pools (**C**) are shown relative to empty vector control, set as 100%. All data are means ± SEM (n=3). *, $P < 0.05$ and **, $P < 0.01$ by Student's _t_-test compared to empty vector.
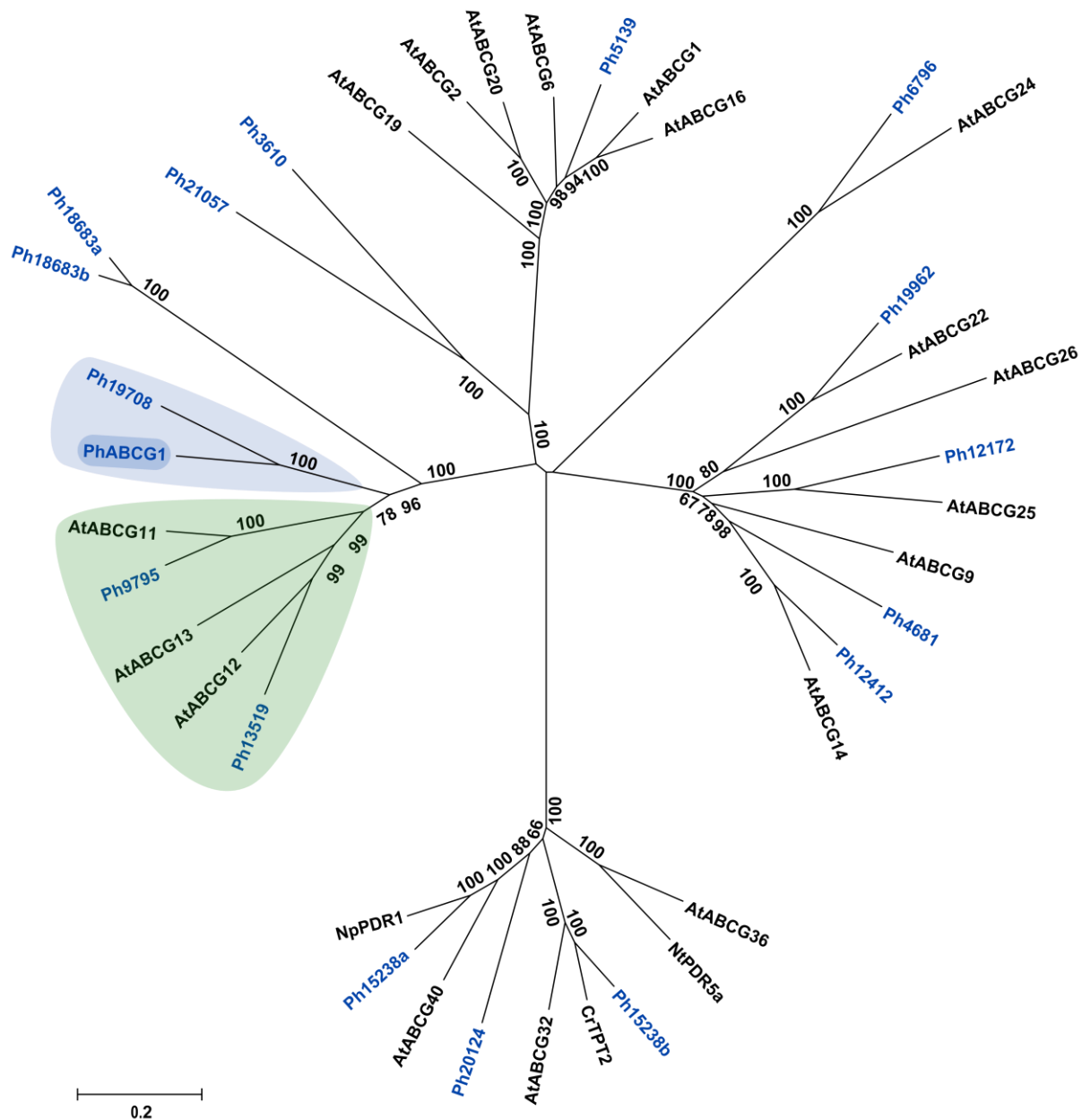
Fig. S10. Neighbor-joining phylogenetic tree including 17 PhABCG transporters expressed in petunia flowers. The phylogenetic tree of 17 PhABCG transporters identified as expressed in petunia flowers by RNAseq (blue text) was drawn using the MEGA 6 software. In addition, 15 *Arabidopsis thaliana* (At) half-size ABCG transporters, for which a function has been identified, were added as well as a few full-size ABCG transporters with known function from *Arabidopsis thaliana*, *Nicotiana plumbaginifolia* (Np), *Nicotiana tabacum* (Nt) and *Catharanthus roseus* (Cr) (black text) as an outgroup to build the tree. The optimal tree with the sum of branch length equal to 11.68655660 is shown. The tree is drawn to scale, with branch lengths in the same units as those of the evolutionary distances used to infer the phylogenetic tree. The scale corresponds to the number of amino acid substitutions per site. Bootstrap percentages higher than 50% are shown (500 iterations). The cluster corresponding to Arabidopsis wax transporters AtABCG11, AtABCG12 and AtABCG13 is highlighted in green and the cluster of PhABCG1 and Ph19708 is shown in blue.
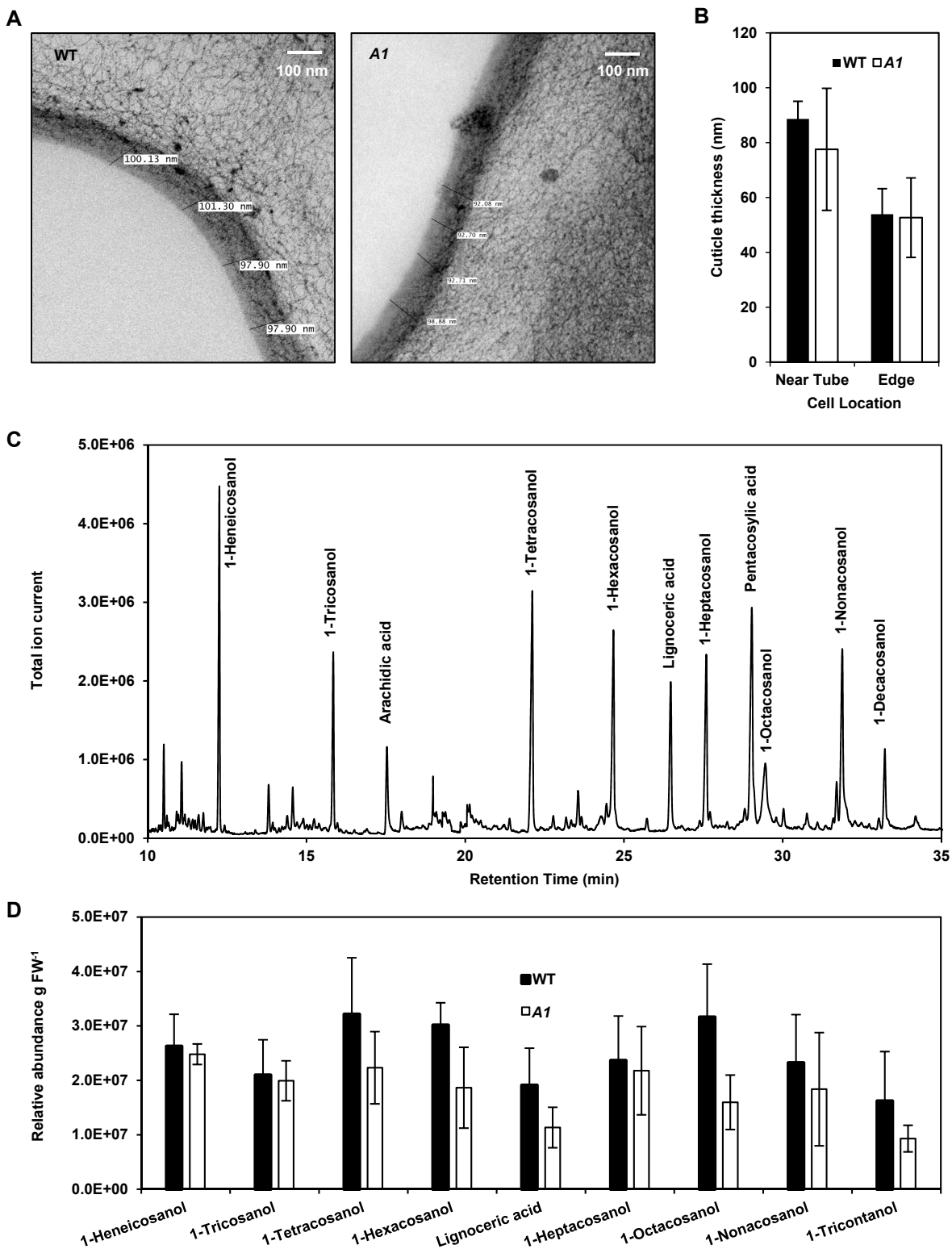
Fig. S11. Effect of *PhABCG1* down-regulation on wax thickness, composition and quantity and in petunia flowers. (A) Representative TEM pictures of cross-sections of wild type (WT) and *PhABCG1*-RNAi *A1* (*A1*) flower epidermal cells. (**B**) Cuticle thickness measured in epidermal cells of WT and *PhABCG1*-RNAi *A1* flowers. Data represent average ± SEM of cuticle thickness of a minimum of 6 cells. From 2 to 7 measurements were taken in multiple locations per individual cell. Student's *t*-test did not show significant difference. (**C**) Representative chromatogram of a derivatized hexane wax extract from petunia flowers analyzed with GC-MS. (**D**) Quantification of the major epicuticular wax alcohols from wild type and *PhABCG1*-RNAi *A1* petunia flowers. Data represent averages ± SD from 3 biological replicates each containing at least 3 flowers.
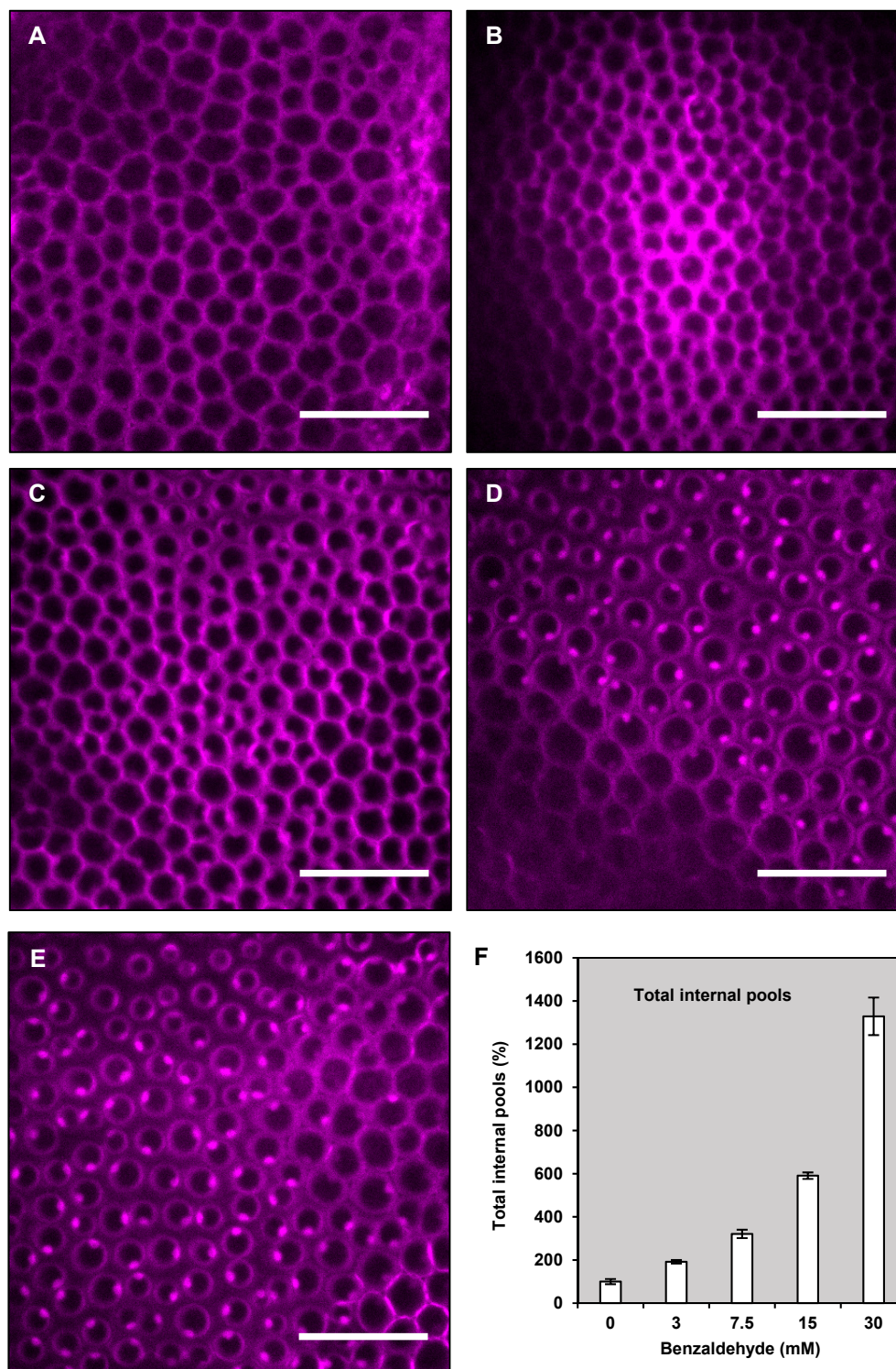
Fig. S12. Mimicking VOC toxicity by feeding wild type petunia petals with a range of concentrations of benzaldehyde. Two-day old wild type petunia petals were fed with benzaldehyde at 0 (**A**), 3 mM (**B**), 7.5 mM (**C**), 15 mM (**D**) and 30 mM (**E**) for 3 hrs with subsequent incubation with propidium iodide for 1 hr. Feeding of benzaldehyde led to an increase in internal pools of volatiles (**F**) due to increase in benzaldehyde, benzyl alcohol, methylbenzoate, and benzylbenzoate. A VOC concentration dependent effect was observed with extensive nuclei staining in 30 mM benzaldehyde-fed flowers, low staining in 15 mM benzaldehyde-fed flowers, and little to no staining after feeding up to 3 mM and 7.5 mM of benzaldehyde. Scale bars are 100 µM.
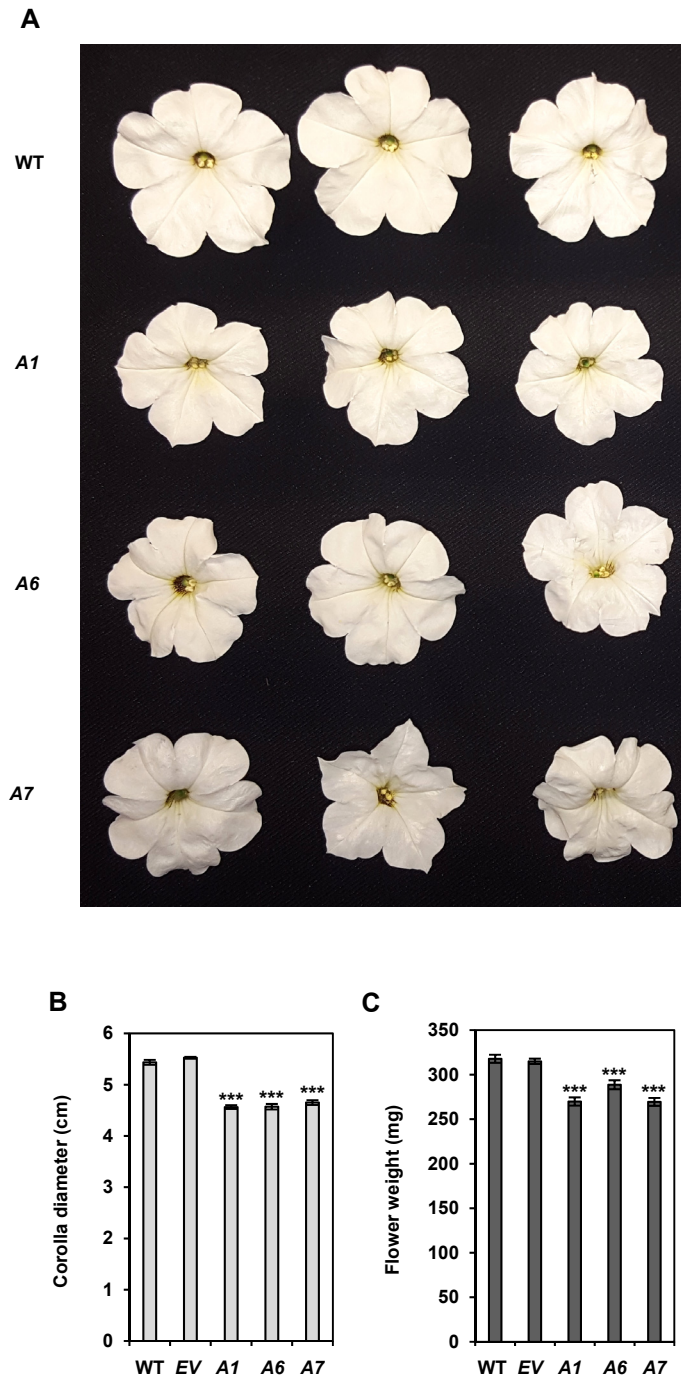
A

B

C

Fig. S13. Effect of *PhABCG1* down-regulation on flower phenotype. (**A**) Representative 1 day old petunia flowers from wild type (WT) and 3 independent *PhABCG1*-RNAi lines (*A1*, *A6* and *A7)*, Data represent (**B**) corolla diameter and (**C**) flower weight from (WT), empty vector (EV) transformed flower and 3 independent *PhABCG1*-RNAi lines (*A1*, *A6* and *A7*) . Data represent averages ± SD, *n* = 40. ***, *P* < 0.001 by Student's *t*-test.
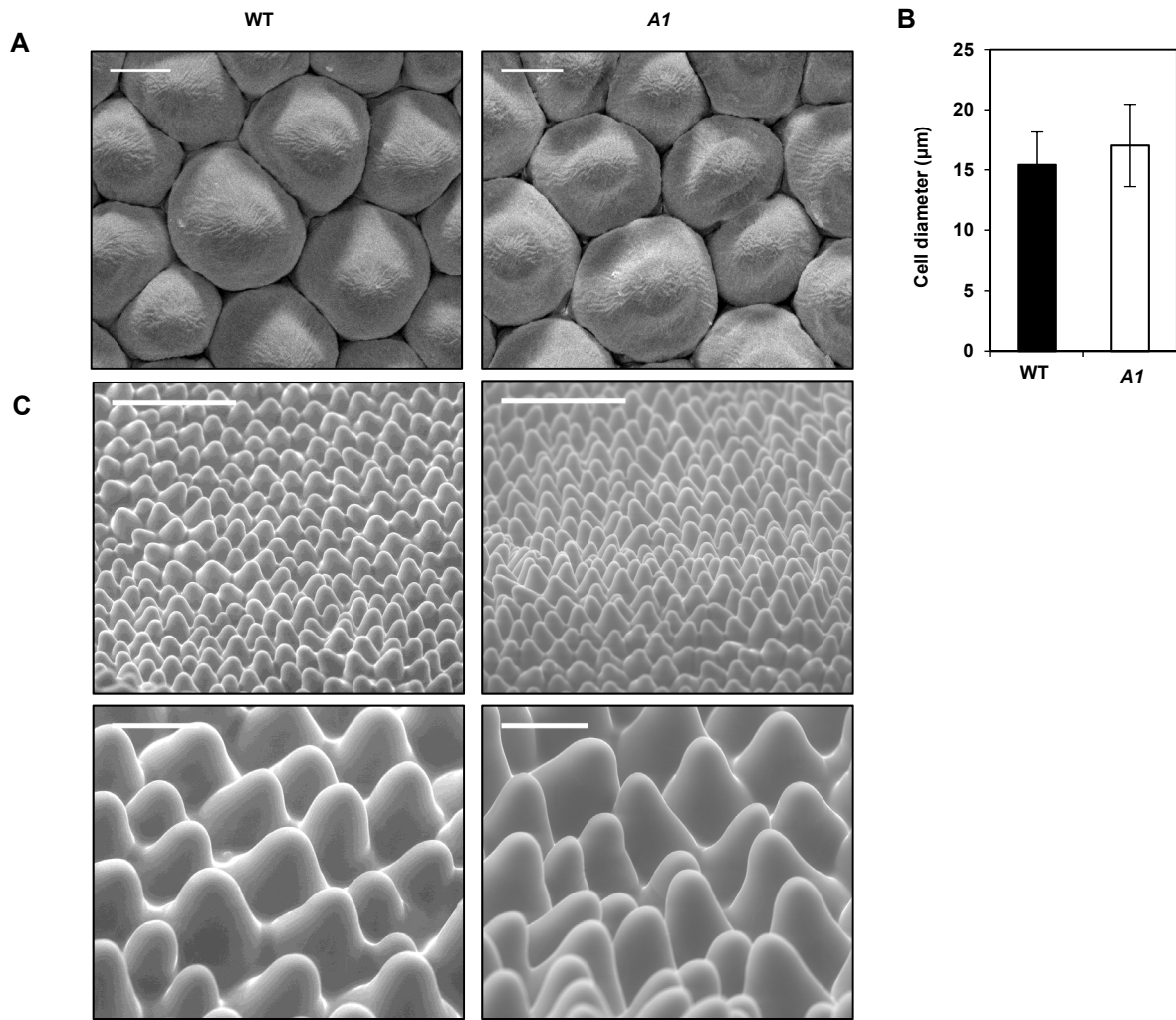
Fig. S14. Effect of *PhABCG1* down-regulation on flower epidermal cell morphology. (**A**) Scanning electron micrograph (SEM) of inner epidermal cells of wild type (WT) and *PhABCG1*-RNAi *A1* petals from flowers 2 days post-anthesis. Scale bar, 10 µm. (**B**) Cell diameter measured at the base of the conical cells shown in (**A**). Data represent averages ± SD, *n*=30. Student's *t*-test did not reveal significant difference in between WT and *A1*. (**C**) Environmental scanning electron micrograph (eSEM) on flower petals. Scale bars, 100µm for upper panel, 20 µm for lower panel.

A

☐ Walker A/P-loop ☐ ABC-transporter signature motif ☐ D-loop
☐ Q-loop ☐ Walker B ☐ H-loop / switch region

1   633 AA

Nuclear Binding Fold   Transmembrane Domains

+H₃N— [yellow bar with domains] α1 α2 α3 α4 α5 α6 —COO⁻   PhABCG1

B

1   559   871   1899 nt

RNAi Target

[blue bar]   *PhABCG1*

ATG   TAG

```
Ph19708   586  ATGTTTCTTGATGAACCAACCAGCGGCCTTGACAGTGCTGCATCTTATTATGTGATGAGT
PhABCG1   559  CTCTTCCTTGATGAACCTACTAGTGGACTTGATAGTGCAGCATCTTATTATGTCATGAAA

Ph19708   646  GGAATTTCACGCCAAAGAGGGGGAAGAACCATTATTGCATCTATTCATCAACCTAGTGCT
PhABCG1   619  GCAATTGCAAGCCAATGCCAAGGGAGAACCATTATTGCCTCAATTCATCAACCTAGTGTT

Ph19708   706  GAAGTTTTCAATCTCTTCCACAATCTGTGCCTTTTGTCTTCTGGAAAAACTGTATATTTT
PhABCG1   679  GACGTTTTCAGTCTGTTTCATTCTTTATGTCTTCTGTCTTCTGGCAGAACTGTGTACTTT

Ph19708   766  GGACCTGCTAGTGCAGCTATTGAGTTTTTCGCGACCAATGGTTTCCCGTGCCCACATCTT
PhABCG1   739  GGCCCTGCTAGTGCAGCAAATGAGTTTTTCGCATTGAGTGGTTTTCCTTGCCCAACTCTC

Ph19708   826  CAAAATCCATCCGATCATTTTCTTAGAACAATAAACCAGGACTTTGTTCATGAGGATCTT
PhABCG1   799  CAGAATCCATCTGATCATTTTCTTAAAAACAATAAACAGTGATTTTGATCAGGACATTGAA

Ph19708   886  GAACAAGGCTCAACTG
PhABCG1   859  GAAGG---TTCAACTA
```

C

(Bar chart: Relative Ph19708 Expression (%) on y-axis from 0 to 120; x-axis categories WT, A1, A6, A7. WT ≈100, A1 ≈105, A6 ≈104, A7 ≈102, all with error bars.)
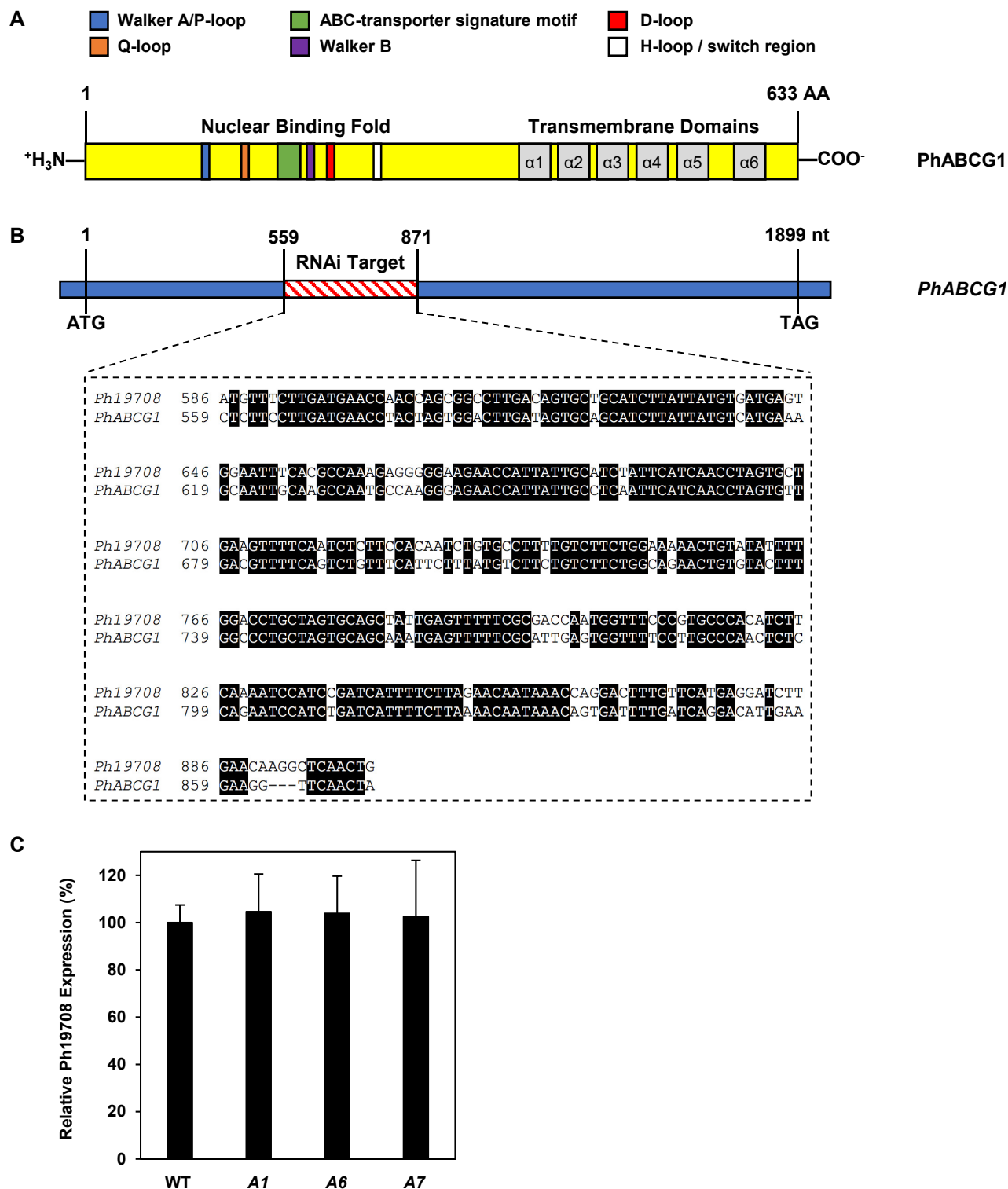
Fig. S15. The *PhABCG1*-RNAi construct specifically triggers down regulation of *PhABCG1*. (A) Schematic presentation of domain arrangements in PhABCG1 protein. **(B)** Diagram depicting location of region used to generate the *PhABCG1* dsRNA trigger and a nucleotide alignment of the *PhABCG1* region targeted by the RNAi trigger with its closest petunia homolog, *Ph19708*. In this region, there is 79% identity between *PhABCG1* and *Ph19708* and no stretch greater than 16 uninterrupted nucleotides is shared between the two expressed genes. **(C)** There is no significant difference in *Ph19708* expression between wild type (WT) and *PhABCG1*-RNAi day 2 flowers. All data are means ± SEM (n=3).

References and Notes

1. J. Peñuelas, J. Llusià, Plant VOC emissions: Making use of the unavoidable. *Trends Ecol. Evol.* **19**, 402–404 (2004). doi:10.1016/j.tree.2004.06.002 Medline

2. N. Dudareva, F. Negre, D. A. Nagegowda, I. Orlova, Plant volatiles: Recent advances and future perspectives. *Crit. Rev. Plant Sci.* **25**, 417–440 (2006). [doi:10.1080/07352680600899973](doi:10.1080/07352680600899973)

3. E. Pichersky, J. Gershenzon, The formation and function of plant volatiles: Perfumes for pollinator attraction and defense. *Curr. Opin. Plant Biol.* **5**, 237–243 (2002). [doi:10.1016/S1369-5266(02)00251-0](doi:10.1016/S1369-5266(02)00251-0) Medline

4. F. Loreto, J. P. Schnitzler, Abiotic stresses and induced BVOCs. *Trends Plant Sci.* **15**, 154–166 (2010). doi:10.1016/j.tplants.2009.12.006 Medline

5. D. F. Zhao, A. Buchholz, R. Tillmann, E. Kleist, C. Wu, F. Rubach, A. Kiendler-Scharr, Y. Rudich, J. Wildt, T. F. Mentel, Environmental conditions regulate the impact of plants on cloud formation. *Nat. Commun.* **8**, 14067 (2017). doi:10.1038/ncomms14067 Medline

6. P. K. Misztal, C. N. Hewitt, J. Wildt, J. D. Blande, A. S. D. Eller, S. Fares, D. R. Gentner, J. B. Gilman, M. Graus, J. Greenberg, A. B. Guenther, A. Hansel, P. Harley, M. Huang, K. Jardine, T. Karl, L. Kaser, F. N. Keutsch, A. Kiendler-Scharr, E. Kleist, B. M. Lerner, T. Li, J. Mak, A. C. Nölscher, R. Schnitzhofer, V. Sinha, B. Thornton, C. Warneke, F. Wegener, C. Werner, J. Williams, D. R. Worton, N. Yassaa, A. H. Goldstein, Atmospheric benzenoid emissions from plants rival those from fossil fuels. *Sci. Rep.* **5**, 12064 (2015). doi:10.1038/srep12064 Medline

7. N. Kolosova, D. Sherman, D. Karlson, N. Dudareva, Cellular and subcellular localization of *S*-adenosyl-L-methionine:benzoic acid carboxyl methyltransferase, the enzyme responsible for biosynthesis of the volatile ester methylbenzoate in snapdragon flowers. *Plant Physiol.* **126**, 956–964 (2001). [doi:10.1104/pp.126.3.956](doi:10.1104/pp.126.3.956) Medline

8. G. Scalliet, C. Lionnet, M. Le Bechec, L. Dutron, J. L. Magnard, S. Baudino, V. Bergougnoux, F. Jullien, P. Chambrier, P. Vergne, C. Dumas, J. M. Cock, P. Hugueney, Role of petal-specific orcinol *O*-methyltransferases in the evolution of rose scent. *Plant Physiol.* **140**, 18–29 (2006). [doi:10.1104/pp.105.070961](doi:10.1104/pp.105.070961) Medline

9. F. Chen, D. K. Ro, J. Petri, J. Gershenzon, J. Bohlmann, E. Pichersky, D. Tholl, Characterization of a root-specific *Arabidopsis* terpene synthase responsible for the formation of the volatile monoterpene 1,8-cineole. *Plant Physiol.* **135**, 1956–1966 (2004). [doi:10.1104/pp.104.044388](doi:10.1104/pp.104.044388) Medline

10. J. J. Glas, B. C. Schimmel, J. M. Alba, R. Escobar-Bravo, R. C. Schuurink, M. R. Kant, Plant glandular trichomes as targets for breeding or engineering of resistance to herbivores. *Int. J. Mol. Sci.* **13**, 17077–17103 (2012). doi:10.3390/ijms131217077 Medline

11. G. Cinege, S. Louis, R. Hänsch, J. P. Schnitzler, Regulation of isoprene synthase promoter by environmental and internal factors. *Plant Mol. Biol.* **69**, 593–604 (2009). [doi:10.1007/s11103-008-9441-2](doi:10.1007/s11103-008-9441-2) Medline

12. U. Niinemets, F. Loreto, M. Reichstein, Physiological and physicochemical controls on foliar volatile organic compound emissions. *Trends Plant Sci.* **9**, 180–186 (2004). doi:10.1016/j.tplants.2004.02.006 Medline

13. U. Niinemets, M. Reichstein, M. Staudt, G. Seufert, J. D. Tenhunen, Stomatal constraints may affect emission of oxygenated monoterpenoids from the foliage of *Pinus pinea*. *Plant Physiol.* **130**, 1371–1385 (2002). doi:10.1104/pp.009670 Medline

14. E. Pichersky, J. P. Noel, N. Dudareva, Biosynthesis of plant volatiles: Nature's diversity and ingenuity. *Science* **311**, 808–811 (2006). doi:10.1126/science.1118510 Medline

15. M. Borghi, A. R. Fernie, F. P. Schiestl, H. J. Bouwmeester, The sexual advantage of looking, smelling, and tasting good: The metabolic network that produces signals for pollinators. *Trends Plant Sci.* **22**, 338–350 (2017). doi:10.1016/j.tplants.2016.12.009 Medline

16. M. C. Schuman, H. A. Valim, Y. Joo, "Temporal dynamics of plant volatiles: Mechanistic bases and functional consequences," in *Deciphering Chemical Language of Plant Communication*, J. D. Blande, R. Glinwood, Eds. (Springer, 2016), pp. 3–34.

17. J. R. Widhalm, R. Jaini, J. A. Morgan, N. Dudareva, Rethinking how volatiles are released from plant cells. *Trends Plant Sci.* **20**, 545–550 (2015). doi:10.1016/j.tplants.2015.06.009 Medline

18. S. A. Mendanha, A. Alonso, Effects of terpenes on fluidity and lipid extraction in phospholipid membranes. *Biophys. Chem.* **198**, 45–54 (2015). doi:10.1016/j.bpc.2015.02.001 Medline

19. H. E. McFarlane, J. J. H. Shin, D. A. Bird, A. L. Samuels, *Arabidopsis* ABCG transporters, which are required for export of diverse cuticular lipids, dimerize in different combinations. *Plant Cell* **22**, 3066–3075 (2010). doi:10.1105/tpc.110.077974 Medline

20. J. Crouzet, J. Roland, E. Peeters, T. Trombik, E. Ducos, J. Nader, M. Boutry, NtPDR1, a plasma membrane ABC transporter from *Nicotiana tabacum*, is involved in diterpene transport. *Plant Mol. Biol.* **82**, 181–192 (2013). doi:10.1007/s11103-013-0053-0 Medline

21. J. R. Widhalm, M. Gutensohn, H. Yoo, F. Adebesin, Y. Qian, L. Guo, R. Jaini, J. H. Lynch, R. M. McCoy, J. T. Shreve, J. Thimmapuram, D. Rhodes, J. A. Morgan, N. Dudareva, Identification of a plastidial phenylalanine exporter that influences flux distribution through the phenylalanine biosynthetic network. *Nat. Commun.* **6**, 8142 (2015). doi:10.1038/ncomms9142 Medline

22. J. C. Verdonk, C. H. Ric de Vos, H. A. Verhoeven, M. A. Haring, A. J. van Tunen, R. C. Schuurink, Regulation of floral scent production in petunia revealed by targeted metabolomics. *Phytochemistry* **62**, 997–1008 (2003). doi:10.1016/S0031-9422(02)00707-0 Medline

23. A. Van Moerkercke, C. S. Galván-Ampudia, J. C. Verdonk, M. A. Haring, R. C. Schuurink, Regulators of floral fragrance production and their target genes in petunia are not exclusively active in the epidermal cells of petals. *J. Exp. Bot.* **63**, 3157–3171 (2012). doi:10.1093/jxb/ers034 Medline

24. J. C. Verdonk, M. A. Haring, A. J. van Tunen, R. C. Schuurink, *ODORANT1* regulates fragrance biosynthesis in petunia flowers. *Plant Cell* **17**, 1612–1624 (2005). doi:10.1105/tpc.104.028837 Medline

25. L. Cseke, N. Dudareva, E. Pichersky, Structure and evolution of linalool synthase. *Mol. Biol. Evol.* **15**, 1491–1498 (1998). doi:10.1093/oxfordjournals.molbev.a025876 Medline

26. S. Mercx, J. Tollet, B. Magy, C. Navarre, M. Boutry, Gene inactivation by CRISPR-Cas9 in *Nicotiana tabacum* BY-2 suspension cells. *Front. Plant Sci.* **7**, 40 (2016). doi:10.3389/fpls.2016.00040 Medline

27. J. Kang, J. Park, H. Choi, B. Burla, T. Kretzschmar, Y. Lee, E. Martinoia, Plant ABC transporters. *Arabidopsis Book* **9**, e0153 (2011). doi:10.1199/tab.0153 Medline

28. N. Rolny, L. Costa, C. Carrión, J. J. Guiamet, Is the electrolyte leakage assay an unequivocal test of membrane deterioration during leaf senescence? *Plant Physiol. Biochem.* **49**, 1220–1227 (2011). doi:10.1016/j.plaphy.2011.06.010 Medline

29. M. Krasnow, M. Matthews, K. Shackel, Evidence for substantial maintenance of membrane integrity and cell viability in normally developing grape (*Vitis vinifera* L.) berries throughout development. *J. Exp. Bot.* **59**, 849–859 (2008). doi:10.1093/jxb/erm372 Medline

30. N. Fernandez-Pozo, H. G. Rosli, G. B. Martin, L. A. Mueller, The SGN VIGS tool: User-friendly software to design virus-induced gene silencing (VIGS) constructs for functional genomics. *Mol. Plant* **8**, 486–488 (2015). doi:10.1016/j.molp.2014.11.024 Medline

31. A. Bombarely, M. Moser, A. Amrad, M. Bao, L. Bapaume, C. S. Barry, M. Bliek, M. R. Boersma, L. Borghi, R. Bruggmann, M. Bucher, N. D'Agostino, K. Davies, U. Druege, N. Dudareva, M. Egea-Cortines, M. Delledonne, N. Fernandez-Pozo, P. Franken, L. Grandont, J. S. Heslop-Harrison, J. Hintzsche, M. Johns, R. Koes, X. Lv, E. Lyons, D. Malla, E. Martinoia, N. S. Mattson, P. Morel, L. A. Mueller, J. Muhlemann, E. Nouri, V. Passeri, M. Pezzotti, Q. Qi, D. Reinhardt, M. Rich, K. R. Richert-Pöggeler, T. P. Robbins, M. C. Schatz, M. E. Schranz, R. C. Schuurink, T. Schwarzacher, K. Spelt, H. Tang, S. L. Urbanus, M. Vandenbussche, K. Vijverberg, G. H. Villarino, R. M. Warner, J. Weiss, Z. Yue, J. Zethof, F. Quattrocchio, T. L. Sims, C. Kuhlemeier, Insight into the evolution of the Solanaceae from the parental genomes of *Petunia hybrida*. *Nat. Plants* **2**, 16074 (2016). doi:10.1038/nplants.2016.74 Medline

32. S. Parrish, J. Fleenor, S. Xu, C. Mello, A. Fire, Functional anatomy of a dsRNA trigger: Differential requirement for the two trigger strands in RNA interference. *Mol. Cell* **6**, 1077–1087 (2000). doi:10.1016/S1097-2765(00)00106-4 Medline

33. G. Segal, R. Song, J. Messing, A new opaque variant of maize by a single dominant RNA-interference-inducing transgene. *Genetics* **165**, 387–397 (2003). Medline

34. A. P. Gleave, A versatile binary vector system with a T-DNA organisational structure conducive to efficient integration of cloned DNA into the plant genome. *Plant Mol. Biol.* **20**, 1203–1207 (1992). doi:10.1007/BF00028910 Medline

35. R. B. Horsch, J. E. Fry, N. L. Hoffmann, D. Eichholtz, S. G. Rogers, R. T. Fraley, A simple and general method for transferring genes into plants. *Science* **227**, 1229–1231 (1985). doi:10.1126/science.227.4691.1229 Medline

36. A. Klempien, Y. Kaminaga, A. Qualley, D. A. Nagegowda, J. R. Widhalm, I. Orlova, A. K. Shasany, G. Taguchi, C. M. Kish, B. R. Cooper, J. C. D'Auria, D. Rhodes, E. Pichersky, N. Dudareva, Contribution of CoA ligases to benzenoid biosynthesis in petunia flowers. *Plant Cell* **24**, 2015–2030 (2012). doi:10.1105/tpc.112.097519 Medline

37. N. Dudareva, L. M. Murfitt, C. J. Mann, N. Gorenstein, N. Kolosova, C. M. Kish, C. Bonham, K. Wood, Developmental regulation of methyl benzoate biosynthesis and emission in snapdragon flowers. *Plant Cell* **12**, 949–961 (2000). doi:10.1105/tpc.12.6.949 Medline

38. I. Orlova, A. Marshall-Colón, J. Schnepp, B. Wood, M. Varbanova, E. Fridman, J. J. Blakeslee, W. A. Peer, A. S. Murphy, D. Rhodes, E. Pichersky, N. Dudareva, Reduction of benzenoid synthesis in petunia flowers reveals multiple pathways to benzoic acid and enhancement in auxin transport. *Plant Cell* **18**, 3458–3475 (2006). doi:10.1105/tpc.106.046227 Medline

39. M. Yanagisawa, A. S. Desyatova, S. A. Belteton, E. L. Mallery, J. A. Turner, D. B. Szymanski, Patterning mechanisms of cytoskeletal and cell wall systems during leaf trichome morphogenesis. *Nat. Plants* **1**, 15014 (2015). doi:10.1038/nplants.2015.14 Medline

40. J. Boatright, F. Negre, X. Chen, C. M. Kish, B. Wood, G. Peel, I. Orlova, D. Gang, D. Rhodes, N. Dudareva, Understanding in vivo benzenoid metabolism in petunia petal tissue. *Plant Physiol.* **135**, 1993–2011 (2004). doi:10.1104/pp.104.045468 Medline

41. I. J. W. M. Goderis, M. F. C. De Bolle, I. E. J. A. François, P. F. J. Wouters, W. F. Broekaert, B. P. A. Cammue, A set of modular plant transformation vectors allowing flexible insertion of up to six expression units. *Plant Mol. Biol.* **50**, 17–27 (2002). doi:10.1023/A:1016052416053 Medline

42. B. De Muynck, C. Navarre, Y. Nizet, J. Stadlmann, M. Boutry, Different subcellular localization and glycosylation for a functional antibody expressed in *Nicotiana tabacum* plants and suspension cells. *Transgenic Res.* **18**, 467–482 (2009). doi:10.1007/s11248-008-9240-1 Medline

43. T. Nagata, Y. Nemoto, S. Hasezawa, Tobacco BY-2 cell line as the "HeLa" cell in the cell biology of higher plants. *Int. Rev. Cytol.* **132**, 1–30 (1992). doi:10.1016/S0074-7696(08)62452-3

44. M. Niczyj, A. Champagne, I. Alam, J. Nader, M. Boutry, Expression of a constitutively activated plasma membrane H$^+$-ATPase in *Nicotiana tabacum* BY-2 cells results in cell expansion. *Planta* **244**, 1109–1124 (2016). doi:10.1007/s00425-016-2571-x Medline

45. M. Jasiński, Y. Stukkens, H. Degand, B. Purnelle, J. Marchand-Brynaert, M. Boutry, A plant plasma membrane ATP binding cassette-type transporter is involved in antifungal terpenoid secretion. *Plant Cell* **13**, 1095–1107 (2001). doi:10.1105/tpc.13.5.1095 Medline

46. C. Larsson, S. Widell, P. Kjellbom, Preparation of high-purity plasma membranes. *Methods Enzymol.* **148**, 558–568 (1987). doi:10.1016/0076-6879(87)48054-3

47. F. Toussaint, B. Pierman, A. Bertin, D. Lévy, M. Boutry, Purification and biochemical characterization of NpABCG5/NpPDR5, a plant pleiotropic drug resistance transporter

expressed in *Nicotiana tabacum* BY-2 suspension cells. *Biochem. J.* **474**, 1689–1703 (2017). doi:10.1042/BCJ20170108 Medline

48. H. Yoo, J. R. Widhalm, Y. Qian, H. Maeda, B. R. Cooper, A. S. Jannasch, I. Gonda, E. Lewinsohn, D. Rhodes, N. Dudareva, An alternative pathway contributes to phenylalanine biosynthesis in plants via a cytosolic tyrosine:phenylpyruvate aminotransferase. *Nat. Commun.* **4**, 2833 (2013). doi:10.1038/ncomms3833 Medline

49. H. Y. Wetzstein, N. Ravid, E. Wilkins, A. P. Martinelli, A morphological and Histological characterization of bisexual and male flower types in pomegranate. *J. Am. Soc. Hortic. Sci.* **136**, 83–92 (2011).

50. K. Tamura, G. Stecher, D. Peterson, A. Filipski, S. Kumar, MEGA6: Molecular Evolutionary Genetics Analysis version 6.0. *Mol. Biol. Evol.* **30**, 2725–2729 (2013). doi:10.1093/molbev/mst197 Medline